Optical and Quantum Electronics (2024) 56:1379
https://doi.org/10.1007/s11082-024-07291-w

# Soliton dynamics and chaotic analysis of the Biswas–Arshed model

**Abdul Hamid Ganie[1] · Mashael M. AlBaidani[2] · Abdul-Majid Wazwaz[3] · Wen-Xiu Ma[4,5,6,7] · Umme Shamima[8] · Mohammad Safi Ullah[8]**

Received: 15 March 2024 / Accepted: 17 July 2024
© The Author(s), under exclusive licence to Springer Science+Business Media, LLC, part of Springer Nature 2024

**Abstract**
In this study, we investigate the Biswas–Arshed (BA) model, applicable in various fields such as fluid mechanics, laser science, and nonlinear optics. We employ the direct algebraic procedure, the modified rational sine–cosine process, and the $\left(\frac{1}{G'}\right)$ approach to obtain soliton dynamics of the mentioned model. Chaotic behavior and sensitivity analysis of the BA model are also investigated using a planar dynamic system. As a result, periodic, quasi-periodic, and chaotic patterns are obtained from the suggested nonlinear model. We also obtain various soliton solutions from this model with novel properties. From the proposed equation, we can obtain periodic waves with bright solitons, bright-dark solitons, dark solitons, breather waves with singularities, double periodic waves, periodic waves with singularities, bright solitons with singularities, multiple bright dark breather waves with singularities, and multiple bright breather waves with singularities. Certain features of the outcomes are exhibited in 2D, 3D, and density views. The work presented is innovative as it offers valuable insights into the governing model's intricate behaviors and diverse waveforms through extensive analysis. This study also contributes to understanding real-world problems by incorporating waveform properties, bifurcation analysis, chaotic dynamics, and sensitivity tests.

**Keywords** Direct algebraic procedure · Modified rational sine–cosine process · $\left(\frac{1}{G'}\right)$-approach · Sensitivity analysis · Optical soliton

## 1 Introduction

Solitons (Ullah 2023; Ullah et al. 2024a) are optical fields that remain unchanged during transmission because of a delicate balance between linear and nonlinear impacts in the system (Ullah et al. 2024b; Ganie et al. 2024). Solitons are essential to modern communication technologies, optical computing, and optical switching. The usage of optical solitons is increasing, mainly with the latest technological advancements. Hence, discussing the optical soliton of a nonlinear partial differential equation became an intimate context. Tappert and Hasegawa first introduced the concept of optical soliton both in

Extended author information available on the last page of the article

normal and anomalous dispersions in 1973 (Hasegawa and Tappert 1973). Different types of models emerge in nonlinear science, for example, the Heisenberg ferromagnetic spin chain model (Salahshour et al. 2021; Kumar and Niwas 2023a), the Boiti–Leon–Manna–Pempinelli equation (Kumar and Niwas 2023b), the Phi-4 model (Roshid et al. 2022), the Klein–Gordon model (Roshid et al. 2023a), the Oskolkov model (Roshid et al. 2023b), the Kudryashov–Sinelshchikov equation (Kumar et al. 2022), the generalized Benjamin–Ono equation (Niwas and Kumar 2023), the Fokas–Lenells model (Ullah et al 2023a), the Zoomeron model (Ullah et al 2023b), the generalized Camassa–Holm Kadomtsev–Petviashvili model (Chen and Guan 2021), the Toda lattice equation (Ma and Maruno 2004), the Kundu–Eckhaus equation (Kudryashov 2020), the Biswas–Arshed model (Aouadi et al. 2019; Mawa et al. 2023; Ullah et al. 2022), the Korteweg–de Vries equation (Zhou et al 2001), the Davey–Stewartson equation (Ma 2004), The Bogoyavlenskii equation model (Uddin et al. 2023), etc. Biswas and Arshed developed an eminent model called the Biswas–Arshed model in 2018 (Biswas and Arshed 2018). This model is applied to the signal transmission through an optical fiber. In this model, there are two types of nonlinear forms. They are power law and Kerr law. The impressive phenomena of this nonlinear problem are the lack of self-phase modulation and a small amount of group velocity dispersion. Another observable phenomenon in this model is the balance of low-group velocity dispersion. Numerous credible and efficient processes have been implemented to elicit the soliton outcome of the BA equation. Sabi'u and his coauthors obtained new exact soliton solutions for studying soliton properties in optical fibers (Sabi'u et al. 2019). Ekici and others found the model's singular, dark, and bright soliton outcomes using the extended trial function algorithm (Ekici and Sonmezoglu 2019). Rehman and his colleagues discovered soliton solutions of the suggested equation by mapping technique (Rehman et al. 2019a). The prime object of this document is to unravel the Kerr law nonlinearity of the BA equation by the direct algebraic technique (Taghizadeh et al. 2012), the modified rational sine–cosine process (Marwan 2022; Akter et al. 2024), and the $\left(\frac{1}{G'}\right)$ approach (Yokus and Durur 2020). Furthermore, this model's chaotic behavior and sensitivity analysis are also investigated using the planar dynamic system. To our consciousness, the Kerr law nonlinearity of the BA equation by our suggested methods has not been published previously.

The arrangement of this paper is expressed in the subsequent form. Section 2 represents the governing model and its ordinary differential structure. The use of the direct algebraic technique is contained in Sect. 3. Section 4 presents the modified rational sine–cosine technique and its utilization. Utilization of the $\left(\frac{1}{G'}\right)$ scheme is discussed in Sect. 5. Section 6 covers the graphical analysis of the outcomes. The chaotic nature of the governing model is described in Sect. 7. Section 8 contains the sensitivity analysis of the suggested nonlinear problem. The result's novelty is presented in Sect. 9. Some concluding notes are provided in Sect. 10.

## 2 Governing model and its ordinary differential form

Let the Biswas–Arshed model be assumed in the following manner (Biswas and Arshed 2018; Sabi'u et al. 2019; Ekici and Sonmezoglu 2019; Rehman et al. 2019a)

$$i\varphi_t + m_1\varphi_{xx} + m_2\varphi_{xt} + i\left(n_1\varphi_{xxx} + n_2\varphi_{xxt}\right) = i\left[s\left(|\varphi|^2\right)\varphi + q\left(|\varphi|^2\right)_x\varphi + v|\varphi|^2\varphi_x\right], \quad (1)$$

where $\varphi$ means the wave function. $x$ and $t$ correspond to the distance and temporal coordinates, sequentially. The first expression of the above equation implies the temporal evolution of solitons whereas $m_1$ premises the coefficient of group velocity dispersion (GVD), $m_2$ premises spatio-temporal dispersion (STD). Moreover, $n_1$ and $n_2$ indicate the third-order dispersion (3OD) and third-order STD, sequentially. The non-linear effect stalk from the coefficients $s$, $q$, and $v$, whereas $p$ gives the self-steepening effect with nonlinear dispersion $q$ and $v$.

Here we will get the ordinary differential equation of the BA model. To obtain it, we assume a transformation form as follows

$$\varphi(x,t) = U(\lambda)e^{i\theta},\ \lambda = x - ct,\ \theta = -ax + bt + e, \tag{2}$$

where $U$ = magnitude of soliton, $c$ = speed of soliton, $\theta$ = phase component, $a$ = soliton frequency, $b$ = number of wave, $e$ = phase constant.

From equations Eq. (1) and Eq. (2), one can reach

$$\left(m_1 - m_2 c + 3n_1 a - 2n_2 ac - n_2 b\right)U'' - (m_1 a^2 - m_2 ab + n_1 a^3 - n_2 a^2 b + b)U - a(s+v)U^3 = 0. \tag{3}$$

## 3 Application of direct algebraic technique

The initial solution of equation Eq. (3) is assumed as (Taghizadeh et al. 2012)

$$U(\lambda) = \sum_{k=0}^{N} l_k \gamma(\lambda), \tag{4}$$

where $l_k$, $(k = 0,1,2,\ldots\ldots\ldots N)$ are free constants and $\gamma$ gratifies the subsequent auxiliary ordinary differential form

$$\gamma'(\lambda) = \gamma^2(\lambda) + M. \tag{5}$$

From Eq. (5), we obtain the following solutions:

$$\gamma(\lambda) = \begin{cases} -\sqrt{-M}tanh\left(\sqrt{-M}\lambda\right), & M < 0, \\ -\sqrt{-M}coth\left(\sqrt{-M}\lambda\right), & M < 0, \end{cases} \tag{6}$$

$$\gamma(\lambda) = \begin{cases} \sqrt{M}tan\left(\sqrt{-M}\lambda\right), & M > 0, \\ -\sqrt{M}cot\left(\sqrt{-M}\lambda\right), & M > 0, \end{cases} \tag{7}$$

$$\gamma(\lambda) = -\frac{1}{\lambda}, M = 0. \tag{8}$$

We can notice the integer $N = 1$ by taking the homogeneous balance between $U^3$ and $U''$ in Eq. (3). For $N = 1$ Eq. (4) becomes

$$U(\lambda) = l_0 + l_1\gamma(\lambda). \tag{9}$$

Now combining Eq. (9) and Eq. (5) and put into Eq. (3), we get the solution as,

$$\begin{aligned} M &= -\frac{a^3n_1 - a^2bn_2 + a^2m_1 - abm_2 + b}{2\left(2can_2 + cm_2 - 3an_1 + bn_2 - m_1\right)},\ l_0 = 0, \\ l_1 &= \pm\sqrt{\frac{-2\left(2can_2 + cm_2 - 3an_1 + bn_2 - m_1\right)}{a(s+v)}}. \end{aligned} \tag{10}$$

Using Eq. (2), and Eqs. (6)-(10), we get,

$\varphi_1(x,t) = -l_1\sqrt{-M}\tanh\left(\sqrt{-M}\lambda\right)e^{i\theta}$,

$\varphi_2(x,t) = -l_1\sqrt{-M}\coth\left(\sqrt{-M}\lambda\right)e^{i\theta}$,

$\varphi_3(x,t) = l_1\sqrt{-M}\tan\left(\sqrt{-M}\lambda\right)e^{i\theta}$,

$\varphi_4(x,t) = -l_1\sqrt{-M}\cot\left(\sqrt{-M}\lambda\right)e^{i\theta}$,

$\varphi_5(x,t) = -\frac{1}{\lambda}l_1e^{i\theta}$,

where $\lambda = x - ct$, $\theta = -ax + bt + e$, $M = -\frac{a^3n_1 - a^2bn_2 + a^2m_1 - abm_2 + b}{2\left(2can_2 + cm_2 - 3an_1 + bn_2 - m_1\right)}$ and $l_1 = \pm\sqrt{\frac{-2\left(2can_2 + cm_2 - 3an_1 + bn_2 - m_1\right)}{a(s+v)}}$.

## 4 Application of modified rational sine–cosine technique

The trial solution of Eq. (3) is (Marwan 2022; Akter et al. 2024)

$$U(\lambda) = \frac{1 + \alpha\sin(\lambda)}{\beta + \gamma\cos(\lambda)}. \tag{11}$$

Then combining Eq. (11) and Eq. (3) and let each coefficient of 1, $\sin(\lambda)$, $\cos(\lambda)$ to zero. Then we obtain the solution sets as:

$$\begin{cases} \alpha = \pm 1, \beta = 0, a = a, \gamma = \pm\sqrt{\frac{as+av}{a^3n_1 - a^2bn_2 + a^2m_1 - abm_2 + b}}, \\ c = -\frac{2a^3n_1 - 2a^2bn_2 + 2a^2m_1 - 2abm_2 - 3an_1 + bn_2 + 2b - m_1}{2an_2 + m_2}, \end{cases} \tag{12}$$

$$\begin{cases} \alpha = \pm\gamma\sqrt{\dfrac{a^3n_1 - a^2bn_2 + a^2m_1 - abm_2 + b}{as + av}}, a = a, \gamma = \gamma, \\ c = -\dfrac{2a^3n_1 - 2a^2bn_2 + 2a^2m_1 - 2abm_2 - 3an_1 + bn_2 + 2b - m_1}{2an_2 + m_2}, \\ \beta = \pm\sqrt{\dfrac{\gamma^2a^3n_1 - \gamma^2a^2bn_2 + \gamma^2a^2m_1 - \gamma^2abm_2 + \gamma^2b - as - av}{a^3n_1 - a^2bn_2 + a^2m_1 - abm_2 + b}}. \end{cases} \tag{13}$$

Combining Eq. (2), Eq. (11), Eq. (12) we get the solution as:

$$\varphi_6(x,t) = \frac{1 \pm \sin(x-ct)}{\gamma \cos(x-ct)} e^{i(-ax+bt+e)}, \tag{14}$$

where $\gamma = \pm\sqrt{\frac{as+av}{a^3n_1-a^2bn_2+a^2m_1-abm_2+b}}$ and $c = -\frac{2a^3n_1-2a^2bn_2+2a^2m_1-2abm_2-3an_1+bn_2+2b-m_1}{2an_2+m_2}$ with arbitrary constant $a$.

Combining Eq. (2), Eq. (11), Eq. (13) we get the solution sets:

$$\varphi_7(x,t) = \frac{1 + \alpha \sin(x-ct)}{\beta + \gamma \cos(x-ct)} e^{i(-ax+bt+e)}, \tag{15}$$

where $\alpha = \pm\gamma\sqrt{\frac{a^3n_1-a^2bn_2+a^2m_1-abm_2+b}{as+av}}$, $\beta = \pm\sqrt{\frac{\gamma^2a^3n_1-\gamma^2a^2bn_2+\gamma^2a^2m_1-\gamma^2abm_2+\gamma^2b-as-av}{a^3n_1-a^2bn_2+a^2m_1-abm_2+b}}$, and $c = -\frac{2a^3n_1-2a^2bn_2+2a^2m_1-2abm_2-3an_1+bn_2+2b-m_1}{2an_2+m_2}$ with arbitrary constants $a$ and$\gamma$.

## 5 Application of $\left(\frac{1}{G'}\right)$ expansion technique

The initial solution of Eq. (3) is (Yokus and Durur 2020)

$$U(\lambda) = \sum_{k=0}^{N} l_k \left(\frac{1}{G'(\lambda)}\right)^k, \tag{16}$$

$$G''(\lambda) + \alpha G'(\lambda) + \beta = 0, \tag{17}$$

where $\alpha$ and $\beta$ are arbitrary components.

From Eq. (14) we get the following context:

$$\frac{1}{G'(\lambda)} = \frac{1}{-\frac{\beta}{\alpha} + A\cosh(\lambda\alpha) - A\sinh(\lambda\alpha)}, \tag{18}$$

where $A$ is a physical constant. We can be noticed integer $N = 1$ by taking the homogeneous balance between $U^3$ and $U''$. For $N = 1$, Eq. (13) becomes

$$U(\lambda) = l_0 + l_1\left(\frac{1}{G'(\lambda)}\right). \tag{19}$$

Now combining Eq. (15), and Eq. (16) and put into Eq. (3) we get the following solution set as

$$\begin{aligned} c = {} & \frac{1}{a^2\left(a^2n_2 + aa^2m_2 - 1\right)\left(2an_2 + m_2\right)}\left(2a^3\alpha^2n_1n_2 - 2a^3sn_2l_0^2 - 2a^3vn_2l_0^2 - aa^2sn_2l_0^2\right. \\ & -a\alpha^2vn_2l_0^2 + 3\alpha^2a^2m_2n_1 - 2a^2vm_2l_0^2 + a\alpha^2m_1m_2 - 3a\alpha^2n_1 + 2a\alpha^2n_1 + 2asl_0^2 \\ & \left. + 2avl_0^2 - \alpha^2m_1\right), a = a,\ \alpha = \alpha,\ \beta = \beta,\ l_0 = l_0, \\ b = {} & \frac{a\left(a^2n_1 + sl_0^2 + vl_0^2 + am_1\right)}{a^2n_2 + am_2 - 1}, l_1 = \frac{2l_0\beta}{\alpha}. \end{aligned} \tag{20}$$

Now utilizing Eq. (16), Eq. (18), and Eq. (19) and put into Eq. (2) we get the solution as,

$$\varphi_8(x,t) = \left(l_0 + \frac{l_1}{-\frac{\beta}{\alpha}+A\cosh((x-ct)\alpha)-A\sinh((x-ct)\alpha)}\right)e^{i(-ax+bt+e)},$$

where $l_1 = \frac{2l_0\beta}{\alpha}$, $b = \frac{a\left(a^2n_1+sl_0^2+vl_0^2+am_1\right)}{a^2n_2+am_2-1}$,

$$c = \frac{1}{a^2\left(a^2n_2+aa^2m_2-1\right)\left(2an_2+m_2\right)}\left(2a^3\alpha^2n_1n_2 - 2a^3sn_2l_0^2 - 2a^3vn_2l_0^2 - a\alpha^2sn_2l_0^2\right.$$
$$- a\alpha^2vn_2l_0^2 + 3\alpha^2a^2m_2n_1 - 2a^2vm_2l_0^2 + a\alpha^2m_1m_2$$
$$\left.-3a\alpha^2n_1 + 2a\alpha^2n_1 + 2asl_0^2 + 2avl_0^2 - \alpha^2m_1\right)$$

with arbitrary constants $a,\alpha,\beta$, and $l_0$.

## 6 Figure analysis

The graphical representation of the outcome $\varphi_7$ is depicted in Fig. 1a–f. Figure shows that $Re(\varphi_7)$ and $Im(\varphi_7)$ exhibit a periodic wave with bright-dark soliton, when the $|\varphi_7|$ exhibits periodic wave with bright soliton.

The outcomes $\varphi_1$ and $\varphi_3$ exhibit the same wave pattern, which is shown in Fig. 2a–f for $\varphi_3$. Figure displays that $Re(\varphi_3)$ and $Im(\varphi_3)$ exhibit a double periodic wave, while the $|\varphi_3|$ exhibits a dark soliton.

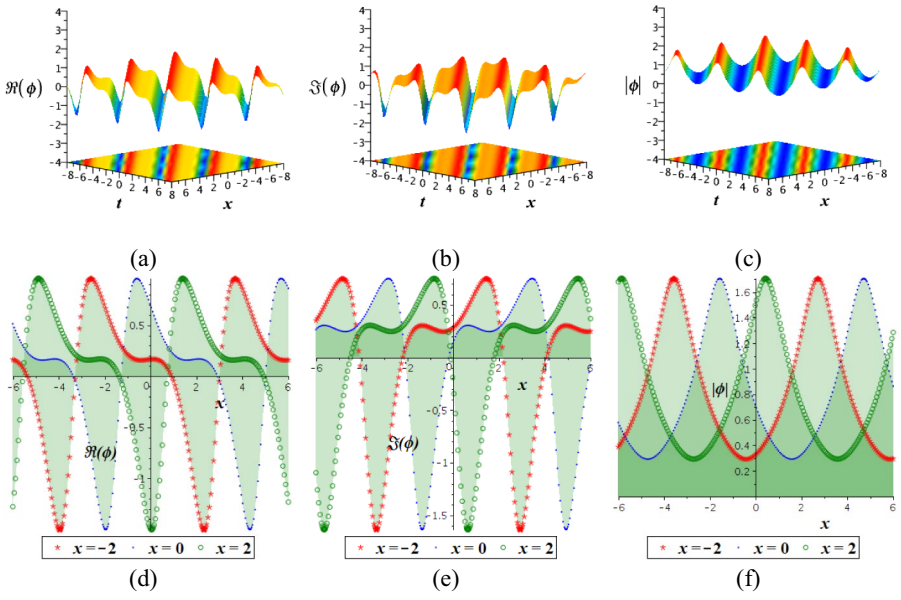


**Fig. 1** Outlook of $\varphi_7$ for $= v = a = b = c = e = \gamma = m_1 = m_2 = n_1 = n_2 = 1$, (a, b, c) 3D with density plot; (d, e, f) 2D plot

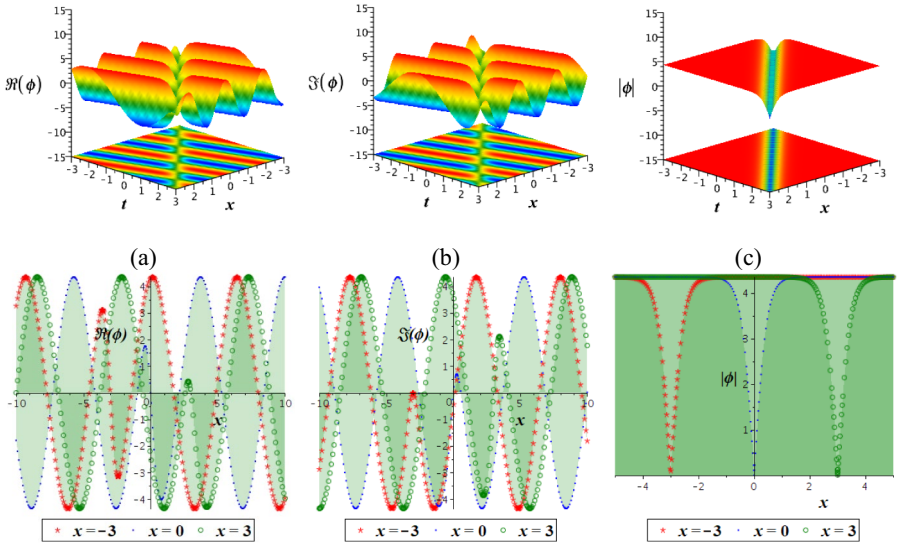


**Fig. 2** Outlook of $\varphi_3$ for $a = m_1 = -3, b = v = c = e = 1, s = 2, m_2 = 3, n_1 = 4, n_2 = 5$, (a, b, c) 3D with density plot; (d, e, f) 2D plot

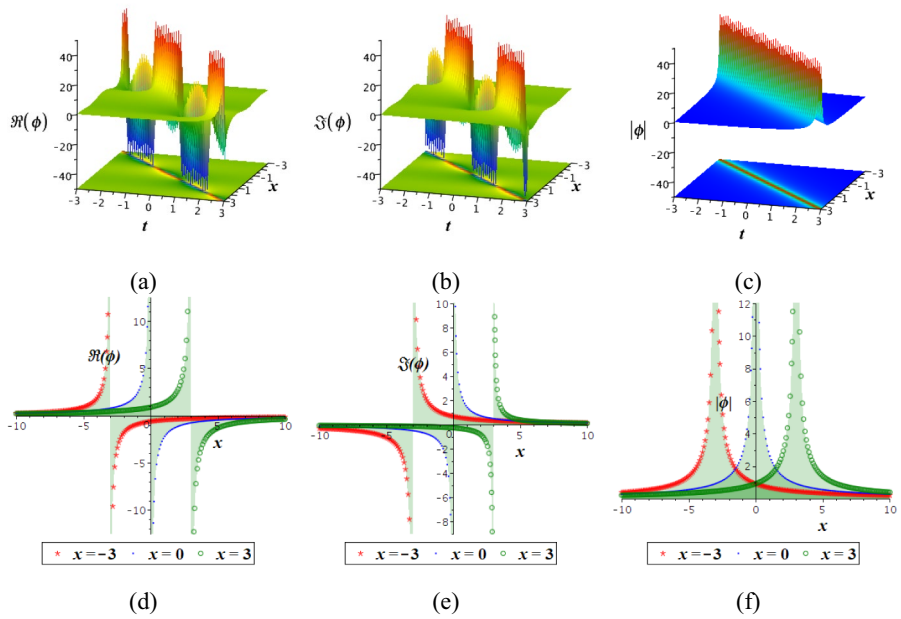


**Fig. 3** Outlook of $\varphi_5$ for $b = n_1 = m_1 = 0, v = c = e = 1, s = a = 2, m_2 = 3, n_2 = 5$ (a, b, c) 3D with density plot; (d, e, f) 2D plot

The outcome $\varphi_5$ is shown in Fig. 3a–f. Figure displays that $Re(\varphi_5)$ and $Im(\varphi_5)$ exhibit a breather wave with singularity, while the $|\varphi_5|$ exhibits a bright soliton with singularity.

The outcomes $\varphi_2$, $\varphi_4$, and $\varphi_8$ exhibit the same wave pattern, which is shown in Fig. 4a–f for $\varphi_2$. One can observe that $Re(\varphi_2)$ and $Im(\varphi_2)$ exhibit a periodic wave with singularity, where $|\varphi_2|$ exhibits a bright soliton with singularity.

The outcome $\varphi_6$ is shown in Fig. 5a–f. Figure displays that $Re(\varphi_6)$ and $Im(\varphi_6)$ exhibit multiple dark-bright breather waves with singularity, while $|\varphi_6|$ exhibits multiple bright breather waves with singularity.

We see that our acquired results contain bright, dark, and bright-dark soliton solutions. It is noted that bright solitons are widely used for long-distance signal transmission without distortion in optical fiber communication networks due to their stable and robust nature. So, it applies to high-speed communication systems (Hasegawa 2022). On the other hand, there are many applications of dark soliton, including all-optical switching, soliton-based logic gates, and fundamental studies of nonlinear dynamics (Kivshar and Davies 1998).

## 7 Chaotic nature

In this section, perturbed terms are used to examine the chaotic nature (Ullah et al. 2024c) of the next dynamical system. Two-dimensional and three-dimensional phase portraits are presented in this investigation. The following dynamical system can be derived from Eq. (3) by setting $\frac{dU}{d\lambda} = H$:

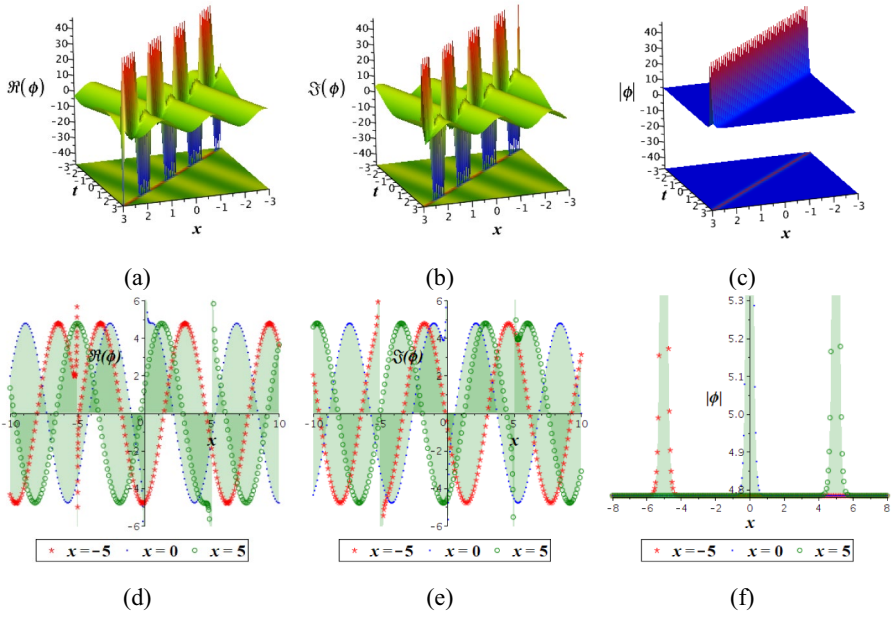


**Fig. 4** Outlook of $\varphi_2$ for $a = m_1 = -3, b = v = c = e = 1, s = 2, m_2 = 3, n_1 = 4, n_2 = 9$, (a, b, c) 3D with density plot; (d, e, f) 2D plot

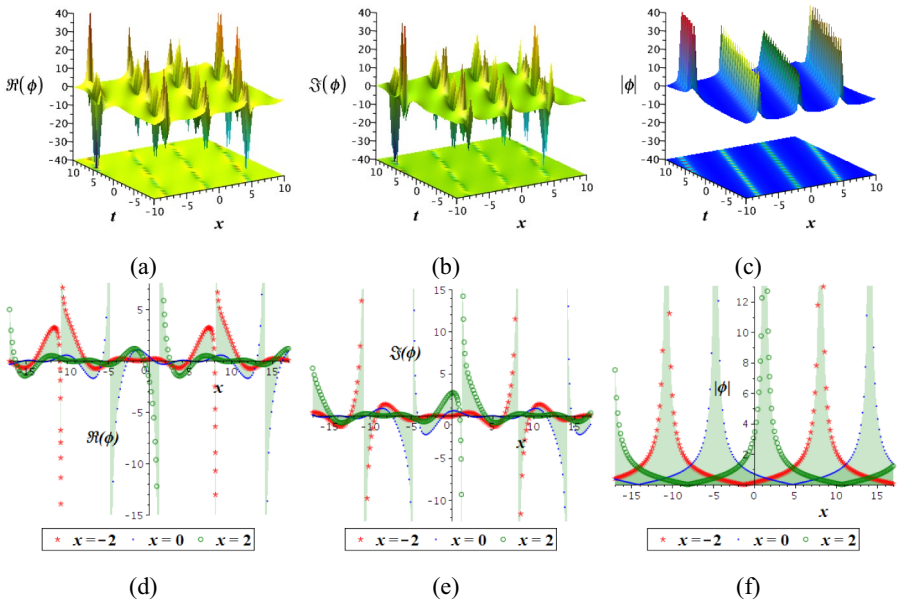


**Fig. 5** Outlook of $\varphi_6$ for $= s = v = a = b = c = e = m_1 = m_2 = n_1 = n_2 = 1$, (a, b, c) 3D with density plot; (d, e, f) 2D plot

$$\frac{dU}{d\lambda} = H, \ \frac{dH}{d\lambda} = -p_1 U - p_2 U^3, \tag{21}$$

where $p_1 = \frac{m_1 a^2 - m_2 ab + n_1 a^3 - n_2 a^2 b + b}{m_1 - m_2 c + 3n_1 a - 2n_2 ac - n_2 b}$ and $p_2 = \frac{a(s+v)}{m_1 - m_2 c + 3n_1 a - 2n_2 ac - n_2 b}$.

Now, equation Eq. (21) includes the additional term $Acos(Bt)$, while $A$ and $B$ are the amplitude and frequency, respectively. Therefore, Eq. (21) will be converted to the following new dynamical system:

$$\frac{dU}{d\lambda} = H, \ \frac{dH}{d\lambda} = -p_1 U - p_2 U^3 + Acos(Bt), \tag{22}$$

Our goal is to determine how perturbation frequency and intensity influence Eq. (22).

Figures 6, 7, and 8 show periodic, quasiperiodic, and chaotic nature for different frequencies and strengths when the key parameters are constant $(b = -3, m_2 = -1, m_1 = n_1 = n_2 = a = s = 1, v = 1.125, c = 7.5)$. Figure 6 indicates the status of Eq. (22) for $A = 0$ with initial value $U(0) = 1$ and $H(0) = 0.1$. The trajectory's status is displayed based on the intensity and frequency of disturbances. In Fig. 6, a time series and phase portraits are shown to illustrate the periodic behavior of Eq. (22). With a small variation in strength and frequency ($A$ and $B$ become 0.2 and 0.3, respectively), Fig. 7 shows a dynamic system changing from a periodic to a quasi-periodic nature with initial value $U(0) = 1$ and $H(0) = 0.1$. In Fig. 8, as the intensity and frequency rise ($A$ and $B$ convert to 2.9 and 3.9, respectively), the system

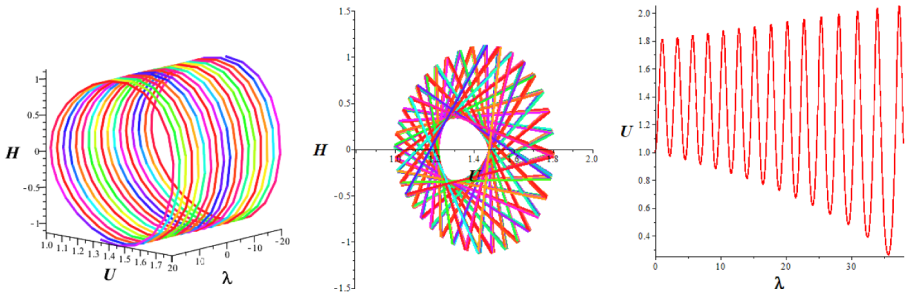


(a) 3D phase diagram (b) 2D phase diagram (c) Time series diagram

**Fig. 6** Periodic nature of system Eq. (22) for $A = 0$, $B = 0$ and $(A(0), B(0)) = (1, 0.1)$

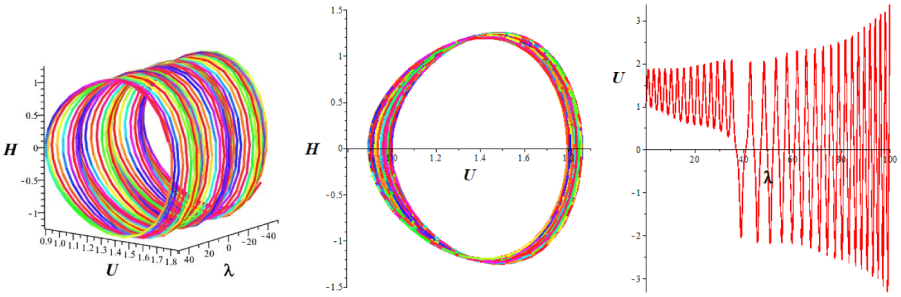


(a) 3D phase diagram (b) 2D phase diagram (c) Time series diagram

**Fig. 7** Quasi-periodic nature of system Eq. (22) for $A = 0.3$, $B = 0.2$ and $(A(0), B(0)) = (1, 0.1)$

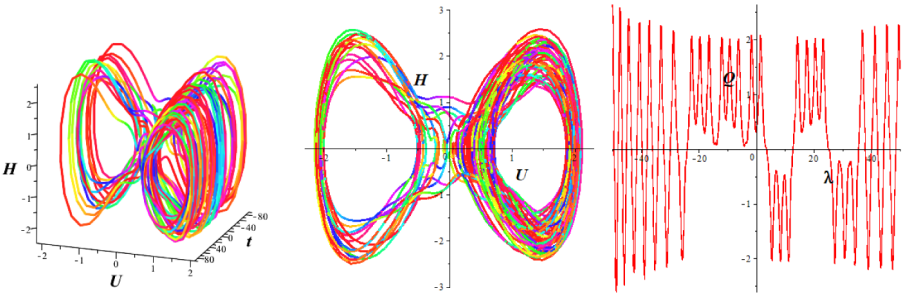


(a) 3D phase diagram (b) 2D phase diagram (c) Time series diagram

**Fig. 8** Chaotic nature of system Eq. (22) for $A = 1.5$, $B = 6$ and $(A(0), B(0)) = (0.3, 0.01)$

experiences turbulent perturbations, shifting into a state of chaos for the initial value $U(0) = 0.3$ and $H(0) = 0.01$.

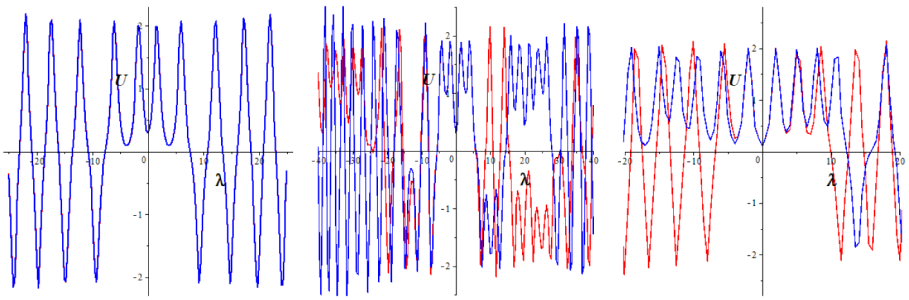


(a) $A = 0, B = 0$ (b) $A = 1.2, B = 3.4$ (c) $A = 1.5, B = 6$

**Fig. 9** Sensitivity diagram of system Eq. (22) for $(A(0), B(0)) = (0.1, 0.01)$ (red curve) and $(A(0), B(0)) = (0.1, 0.02)$ (blue curve)

## 8 Sensitivity analysis

This section investigated the sensitivity analysis (Ullah et al. 2024c) of the perturbed system Eq. (22), examining the effects of initial conditions using constant parameter values $(b = -3, m_2 = -1, m_1 = n_1 = n_2 = a = s = 1, v = 1.125, c = 7.5)$. Based on Fig. 9, we can see a red curve that signifies a time series diagram with an initial value of $(A(0), B(0)) = (0.1, 0.01)$ and a blue curve representing an initial value of $(A(0), B(0)) = (0.1, 0.02)$. From Fig. 9a, we see that the initial value of the perturbed system determines two overlapped periodic waves of the result and the dynamic system is not sensitive ($A = 0$, $B = 0$). The two-time series diagram of Fig. 9b demonstrates low sensitivity is indicated to the initial state when perturbation strength and frequency are small ($A = 1.2$, $B = 3.4$). Furthermore, Fig. 9c displays significant changes between time series diagrams when perturbation strength and frequency rise ($A = 1.5$, $B = 6$), indicating that the time series diagram is more sensitive to variations in initial values when perturbation strength and frequency increase.

## 9 Comparative analysis and novelty of results

From this part, we find the novelty and effectiveness of our proposed model. We have analyzed several papers, which were recently published based on this model. Different types of methods have been employed to solve the BA model. The extended trial function method is applied to find the dark, singular, and bright solitons (Ekici and Sonmezoglu 2019). The mapping method is adopted to acquire the optical soliton outcomes of the mentioned model (Rehman et al. 2019a). The modified mapping and undetermined coefficient methods are utilized to find the singular, singular periodic, dark, bright, and dark-singular mixed solitons (Rehman et al. 2019b). The modified simple equation architecture is implemented to find the optical dark, bright, and singular solitons, singular periodic solutions (Yildirim 2019). We have periodic waves with bright solitons, bright-dark solitons, dark solitons, double periodic waves, periodic waves with singularity, breather waves with singularity, bright solitons with

**Table 1** Comparison of the obtained solutions and existing article (Rehman et al. 2019a)

| If $P = \pm\sqrt{-\frac{2(m_1-m_2c+3n_1a-2n_2ac-n_2b)}{a(s+v)}}$, $Q = x - ct$, $q(x,t) = \varphi(x,t)$, $\lambda = x - ct$, and $\theta = -ax + bt + e$, then | If $P = -l_1\sqrt{-M}$, $Q = \sqrt{-M}(x - ct)$, $\varphi_1(x,t) = \varphi(x,t)$ ,$\theta = -ax + bt + e$, $M = -\frac{a^3n_1-a^2bn_2+a^2m_1-abm_2+b}{2(2can_2+cm_2-3an_1+bn_2-m_1)}$ and $l_1 = \pm\sqrt{\frac{-2(2can_2+cm_2-3an_1+bn_2-m_1)}{a(s+v)}}$, then |
|---|---|
| Rehman et al. solution (17) will be $\varphi(x,t) = \text{Ptanh}(Q)e^{i\theta}$ | For $M < 0$, our solution $\varphi_1(x,t)$ will be $\varphi(x,t) = \text{Ptanh}(Q)e^{i\theta}$, |
| Rehman et al. solution (28) will be $\varphi(x,t) = \text{Pcoth}(Q)e^{i\theta}$ | For $M < 0$, our solution $\varphi_2(x,t)$ will be $\varphi(x,t) = \text{Ptanh}(Q)e^{i\theta}$, |
| Rehman et al. solution (34) will be $\varphi(x,t) = \text{Ptan}(Q)e^{i\theta}$ | For $M > 0$, our solution $\varphi_3(x,t)$ will be $\varphi(x,t) = \text{Ptan}(Q)e^{i\theta}$, |
| Rehman et al. solution (24) will be $\varphi(x,t) = \text{Pcot}(G)e^{i\theta}$ | For $M > 0$, then our solution $\varphi_4(x,t)$ will be $\varphi(x,t) = \text{Pcot}(Q)e^{i\theta}$ |

singularity, multiple dark-bright breather waves with singularity, and multiple bright breather waves with singularity of the Biswas–Arshed model by applying distinct analytical methods. These solutions are more effective and advanced than before. In Table 1, we also compare some of our outcomes with those in (Rehman et al. 2019a). Furthermore, chaos and sensitivity analyses of this model are also investigated using the planar dynamic system, which other studies have not stated.

## 10 Conclusion

In this study, the direct algebraic procedure, the modified rational sine–cosine process, and the $\left(\frac{1}{G'}\right)$-approach has been effectively used to find out the soliton outcomes of the BA equation. Chaotic behavior and sensitivity of this model are also investigated using the planar dynamic system. Consequently, periodic, quasi-periodic, and chaotic patterns are obtained from the suggested nonlinear model. Periodic waves with bright solitons, bright-dark solitons, dark solitons, double periodic waves, breather waves with singularity, periodic waves with singularity, bright solitons with singularity, multiple bright dark breather waves with singularity, and multiple bright breather waves with singularity can also be acquired from the proposed model. Certain features of the acquired outcomes have been exhibited in 2D, 3D, and density views. It is evident from the results that the integration methods employed are powerful, concise, and efficient. Additionally, they suggest that they can be applied to higher-order nonlinear models emerging in modern science and engineering.

**Author contributions** Abdul Hamid Ganie: Methodology, Data curation, Investigation. Mashael M. AlBaidani: Writing–review & editing, Visualization. Abdul-Majid Wazwaz: Conceptualization, Supervision. Wen-Xiu Ma: Supervision, Visualization, Validation. Umme Shamima: Writing—original draft, Software. Mohammad Safi Ullah: Supervision, Writing—review & editing, Investigation.

**Funding** Not applicable.

**Data availability** No datasets were generated or analysed during the current study.

## Declarations

**Conflict of interest** The authors declare no competing interests.

**Ethical Approval** I declare that this study is my work based on the reviewers' suggestions. Other than the quoted contents, this study contains no research achievements that have been previously published or written.

## References


Akter, M., Ullah, M.S., Wazwaz, A.M., Seadawy, A.R.: Unveiling Hirota–Maccari model dynamics via diverse elegant methods. Opt. Quant. Electron. **56**, 6714 (2024)

Aouadi, S., Bouzida, A., Daoui, A.K., Triki, H., Zhou, Q., Liu, S.: W-shaped, bright and dark solitons of Biswas–Arshed equation. Optik **182**, 227–232 (2019)

Biswas, A., Arshed, S.: Optical solitons in presence of higher order dispersions and absence of self-phase modulation. Optik **174**, 452–459 (2018)

Chen, L., Guan, C.: Global solutions for the generalized Camassa–Holm equation. Nonlin Anal **58**, 103227 (2021)

Ekici, M., Sonmezoglu, A.: Optical solitons with Biswas–Arshed equation by extended trial function method. Optik **177**, 13–20 (2019)

Ganie, A.H., Wazwaz, A.M., Seadawy, A.R., Ullah, M.S., Roshid, H.O., Afroz, H.D., Akter, R.: Application of three analytical approaches to the model of ion sound and Langmuir waves. Pramana – J. Phys. **98**, 46 (2024)

Hasegawa, A.: Optical soliton: Review of its discovery and applications in ultra-high-speed communications. Front. Phys. **10**, 1044845 (2022)

Hasegawa, A., Tappert, F.D.: Transmission of stationary nonlinear optical pulses in dispersive dielectric fibers. I. Anomalous Dispersion. Appl Phys Lett **23**(3), 142 (1973)

Kivshar, Y.S., Davies, B.L.: Dark optical solitons: physics and applications. Phys. Rep. **298**(2–3), 81–197 (1998)

Kudryashov, N.A.: On travelling wave solutions of the Kundu–Eckhaus equation. Optik **224**, 165500 (2020)

Kumar, S., Niwas, M.: Exploring lump soliton solutions and wave interactions using new inverse ($G'/G$)-expansion approach: applications to the (2+1)-dimensional nonlinear Heisenberg ferromagnetic spin chain equation. Nonlinear Dyn. **111**, 20257–20273 (2023a)

Kumar, S., Niwas, M.: Analyzing multi-peak and lump solutions of the variable-coefficient Boiti–Leon–Manna–Pempinelli equation: a comparative study of the Lie classical method and unified method with applications. Nonlinear Dyn. **111**, 22457–22475 (2023b)

Kumar, S., Niwas, M., Dhiman, S.K.: Abundant analytical soliton solutions and different wave profiles to the Kudryashov–Sinelshchikov equation in mathematical physics. J. Ocean Eng. Sci. **7**(6), 565–577 (2022)

Ma, W.X.: Wronskians, generalized Wronskians and solutions to the Korteweg-de Vries equation. Chaos Solitons Fract. **19**, 163–170 (2004)

Ma, W.X., Maruno, K.: Complexiton solutions of the Toda lattice equation. Phys. A **343**, 219–237 (2004)

Marwan, A.: New interesting optical solutions to the quadratic-cubic Schrödinger equation by using the Kudryashov-expansion method and the updated rational sine-cosine functions. Op. Quant. Electron. **54**, 666 (2022)

Mawa, H.Z., Islam, S.M.R., Bashar, M.H., Roshid, M.M., Islam, J., Akhter, S.: Soliton solutions to the BA model and (3 + 1)-dimensional KP equation using advanced exp ($-\phi(\xi)$)-expansion scheme in mathematical physics. Math. Probl. Eng. **2023**, 5564509 (2023)

Niwas, M., Kumar, S.: Multi-peakons, lumps, and other solitons solutions for the (2+1)- dimensional generalized Benjamin–Ono equation: an inverse ($G'/G$)-expansion method and real-world applications. Nonlinear Dyn. **111**, 22499–22512 (2023)

Rehman, H.U., Saleem, M.S., Zubair, M., Jafar, S., Latif, I.: Optical solitons with Biswas–Arshed model using mapping method. Optik **194**, 163091 (2019a)

Rehman, H.U., Younis, M., Jafar, S., Tahir, M., Saleem, M.S.: Optical solitons of Biswas–Arshed model in birefrigent fiber without four wave mixing. Optik **213**, 164669 (2019b)

Roshid, M.M., Abdeljabbar, A., Aldurayhim, A., Rahman, M.M., Roshid, H.O., Alshammari, F.S.: Dynamical interaction of solitary, periodic, rogue type wave solutions and multi-soliton solutions of the nonlinear models. Heliyon. **8**(12), e11996 (2022)

Roshid, H.O., Roshid, M.M., Hossain, M.M., Hasan, M.S., Munshi, M.J.H., Sajib, A.H.: Dynamical structure of truncated M−fractional Klein–Gordon model via two integral schemes. Results Phys. **46**, 106272 (2023a)

Roshid, H.O., Roshid, M.M., Abdeljabbar, A., Begum, M., Basher, H.: Abundant dynamical solitary waves through Kelvin–Voigt fluid via the truncated M-fractional Oskolkov model. Results Phys. **55**, 107128 (2023b)

Sabi'u, J., Rezazadeh, H., Tariq, H., Bekir, A.: Optical solitons for the two forms of Biswas–Arshed model. Mod. Phys. Lett. B **33**(25), 1950308 (2019)

Salahshour, S., Hosseini, K., Mirzazadeh, M., Baskonus, H.M.: 1-Soliton solutions of the (2+1)-dimensional Heisenberg ferromagnetic spin chain model with the beta time derivative. Opt. Quant. Electron. **53**, 125 (2021)

Taghizadeh, N., Neirameh, A., Shokooh, S.: New application of direct algebraic method to Eckhaus equation. Trends Appl Sci Res **7**(6), 476–482 (2012)

Uddin, M.S., Begum, M., Roshid, H.O., Ullah, M.S., Abdeljabbar, A.: Soliton solutions of a (2+1)-dimensional nonlinear time-fractional Bogoyavlenskii equation model. Partial Differ. Equ. Appl. Math. **8**, 100591 (2023)

Ullah, M.S.: Interaction solutions to the (3+1)-D negative-order KdV first structure. Partial Differ. Equ. Appl. Math. **8**, 100566 (2023)

Ullah, M.S., Abdeljabbar, A., Roshid, H.O., Ali, M.Z.: Application of the unified method to solve the Biswas–Arshed model. Results Phys. **42**, 105946 (2022)

Ullah, M.S., Roshid, H.O., Ali, M.Z.: New wave behaviors of the Fokas–Lenells model using three integration techniques. PLoS ONE **18**(9), 0283594 (2023a)

Ullah, M.S., Mostafa, M., Ali, M.Z., Roshid, H.O., Akter, M.: Soliton solutions for the Zoomeron model applying three analytical techniques. PLoS ONE **18**(7), e0283594 (2023b)

Ullah, M.S., Ali, M.Z., Roshid, H.O.: Bifurcation analysis and new waveforms to the first fractional WBBM equation. Sci. Rep. **14**, 11907 (2024a)

Ullah, M.S., Roshid, H.O., Ali, M.Z.: New wave behaviors and stability analysis for the (2+1)-dimensional Zoomeron model. Opt. Quant. Electron. **56**, 240 (2024b)

Ullah, M.S., Ali, M.Z., Roshid, H.O.: Bifurcation analysis and new waveforms to the fractional KFG equation. Partial Differ. Equ. Appl. Math. **10**, 100716 (2024c)

Yildirim, Y.: Optical solitons to Biswas–Arshed model in birefringent fibers using modified simple equation architecture. Optik **182**, 1149–1162 (2019)

Yokus, A., Durur, H.: $(1\frac{G'}{})$-expansion method for exact solutions of (3+1)-dimensional Jimbo–Miwa equation. Matematik **10**(4), 2907–2914 (2020)

Zhou, Z.X., Ma, W.X., Zhou, R.G.: Finite-dimensional integrable systems associated with the Davey–Stewartson I equation. Nonlinearity **14**, 701–717 (2001)

**Publisher's Note** Springer Nature remains neutral with regard to jurisdictional claims in published maps and institutional affiliations.

Springer Nature or its licensor (e.g. a society or other partner) holds exclusive rights to this article under a publishing agreement with the author(s) or other rightsholder(s); author self-archiving of the accepted manuscript version of this article is solely governed by the terms of such publishing agreement and applicable law.

## Authors and Affiliations

**Abdul Hamid Ganie[1] · Mashael M. AlBaidani[2] · Abdul-Majid Wazwaz[3] · Wen-Xiu Ma[4,5,6,7] · Umme Shamima[8] · Mohammad Safi Ullah[8]**

✉ Wen-Xiu Ma
mawx@cas.usf.edu

✉ Mohammad Safi Ullah
safi.ru1985@gmail.com

Abdul Hamid Ganie
a.ganie@seu.edu.sa

Mashael M. AlBaidani
m.albaidani@psau.edu.sa

Abdul-Majid Wazwaz
wazwaz@sxu.edu

Umme Shamima
shamimaumme6@gmail.com

[1] Basic Science Department, College of Science and Theoretical Studies, Saudi Electronic University, 11673 Riyadh, Saudi Arabia

[2] Department of Mathematics, College of Science and Humanities, Prince Sattam Bin Abdulaziz University, 11942 Al Kharj, Saudi Arabia

[3] Department of Mathematics, Saint Xavier University, Chicago, IL 60655, USA

[4] Department of Mathematics, Zhejiang Normal University, Jinhua 321004, Zhejiang, China

[5] Department of Mathematics, King Abdulaziz University, 21589 Jeddah, Saudi Arabia

[6] Department of Mathematics and Statistics, University of South Florida, Tampa, FL 33620-5700, USA

[7] Material Science Innovation and Modelling, Department of Mathematical Sciences, North-West University, Mafikeng Campus, Mmabatho 2735, South Africa

[8] Department of Mathematics, Comilla University, Cumilla 3506, Bangladesh